Contract No:

This document was prepared in conjunction with work accomplished under Contract No. DE-AC09-08SR22470 with the U.S. Department of Energy (DOE) Office of Environmental Management (EM).

Disclaimer:

Design and implementation of a data analysis pipeline for paper spray ionization mass spectrometry of UO_2Cl_2

Samuel Koby[1,2], Joseph Mannion[2], Joshua Hewitt[2], Matthew Wellons[2]

[1]Department of Energy, Science Undergraduate Laboratory Internship (SULI) Program

[2]Savannah River National Laboratory, National Security Directorate, Aiken, SC 29808

Ambient mass spectrometry is an emerging characterization method for nuclear materials analysis. SRNL has recently acquired a new JEOL AccuTOF™-DART® LP 4G with a Filter Spray™ front end sample injection system, to develop new methods for ambient mass spectrometry of uranium analytes. Preliminary measurements of uranium-containing samples have demonstrated a need to rapidly evaluate large datasets generated with tailored data analysis scripts. To address this gap a data analysis pipeline written in R within the R Studio environment has been developed. The pipeline comprises a series of processing steps where the data are ingested, analyte peaks of interest are extracted, subsequent ratio and normalization calculations are performed, and results are presented in a series of graphical plots. In detail, the data files containing up to several hundred chronological spectra of a single sample in netCDF format were first extracted into RStudio. Then, initial 3D plots of the data were created in respect to the time, intensity, and mass to charge domains. These graphics serve as an initial easily visualized survey of instrument data. Next, a .csv format file containing the names, masses, and abundances of isotopes of interest were ingested into RStudio and were used to automatically collect intensity values at the mass value. Uranium isotope ratios were plotted against gadolinium isotope ratios (gadolinium was used as an internal standard) and assessed for ion beam stability and intensity. The spectra were filtered by applying a threshold intensity for the $^{158}GdO^+$ mass channel. A Monte Carlo experiment was performed by creating a theoretical distribution of the data in order to determine the ratio of the uranium isotopes. The results show that the developed data analysis pipeline successfully filters high quality data from overall poor quality runs. Our results also support the idea that paper spray ionization mass spectrometry can be used for both detection and quantification of trace amounts of uranium compounds.

INTRODUCTION

Characterization of actinides within environmentally collected samples is paramount for efforts in environmental monitoring,[1, 2] nuclear forensics,[3-5] and nuclear safeguards.[6-8] Various analytical techniques are utilized for these efforts including radiometric techniques (ex. α- and γ-spectroscopy), microscopy based techniques (ex. energy dispersive x-ray microanalysis), and mass spectrometry (ex. multi-collector inductively coup pled plasma mass spectrometry). A shortcoming of current analytical paradigms is the lack of chemical information provided by these analyses. Actinide speciation is lost through harsh sample preparation and instrument conditions (ex. ionization within a plasma torch), or is inherently non-discernable by the technique (ex. γ-spectroscopy or SEM-EDS). The chemical speciation of actinides (or concurrent organic species) can provide clues as to the intent or history of the material, and offers and additional axis for forensic fingerprinting. For example, the presence of uranyl-tributyl phosphate complexes may indicate undisclosed reprocessing efforts,[9] or the state of hydrolysis could be used to determine the age or history of the material.[10] Mass spectrometric techniques have long been recognized as the most sensitive methods for the characterization of long-lived actinides, but these techniques have been utilized primarily for isotope ratio measurements[11, 12] or characterization of inorganic contaminates.[3, 13]

Paper spray ionization mass spectrometry (PSI-MS) has recently gained attention as a versatile technique requiring no sample preparation for the direct analysis of blood,[14-16] urine,[17, 18] and environmentally collected chemical warfare agent simulants.[19] The elimination of sample preparation would strengthen nuclear safeguards in several regards. First, sample turnaround would be greatly expedited, allowing for more timely detection of clandestine activities. Second, chemical information and organics captured on swipes would be preserved, providing additional

clues regarding the operation of a facility or the intended use of material. Third, the reduced cost and time associated with analyses would allow for a greater number of measurements to be conducted, improving the likelihood of the detection of clandestine activities. PSI-MS has several advantages over other comparable analytical techniques (e.g. LC-ESI-MS) including reduced sample preparation, rapid processing, and reduced carryover. Additionally, PSI-MS may be easily be integrated into the current swipe sampling paradigm and chemical speciation is retained as ionization is "soft" and the sample is only solvated immediately prior to analysis, minimizing the potential for in-solution chemical transformations.

PSI-MS generates massive amounts of data, often collecting approximately a spectra per second during the multi-minute long analysis of a single sample. Therefore, the development of a data analysis pipeline in order to rapidly extract meaning from this mountain of data is necessary for the implementation of PSI-MS for the analysis of actinides. Herein we describe the development and implementation of a data analysis pipeline written in R within the RStudio designed to rapidly perform quality control and uranium isotopic analysis on samples containing 50 ppm $GdCl_3$ and varying concentrations of UO_2Cl_2 obtained from a JEOL AccuTOF™-DART® LP 4G with a Filter Spray™ front end sample injection system.

METHODOLOGY

Five netCDF data files containing chronological spectra of samples of 50 ppm $GdCl_3$ as an internal standard and varying concentrations of UO_2Cl_2 at natural enrichment levels on a filter paper substrate were ingested into the RStudio environment using the ncdf4 and MALDIquantForeign packages. Exploratory three-dimensional plots of the data with respect to time, intensity, and mass to charge domains were generated using the plot3D library. A csv file containing the names and literature values of the mass and abundance for $^{238}UO_2^+$, $^{235}UO_2^+$,

$^{158}GdO^{+}$, and $^{160}GdO^{+}$ was then ingested. For each isotope, the maximum intensity value within .3 amu of the literature mass value of each spectrum was extracted using the MALDIquant package and stored in a vector. If no value existed within the allotted range, then it was assigned a "-Inf" value. Each vector was then postprocessed to replace any "-Inf" values with 0. The resulting vectors were stored as a data frame with isotope names as column headers.

Plots of the ratio of the uranyl isotopic ratios versus the gadolinium oxide isotopic ratios were generated as a quality control plot. Lines denoting the ratio of the literature values of the abundance of the isotopes were appended onto the plot. In general, these plots contained a dense mass of data in the vicinity of the intercept of these two lines, along with random data points throughout the remainder of the plot. Inspection of the data in these plots revealed that the points most centered on this intercept tended to have high GdO^{+} intensity. Plots of the intensity of the GdO^{+} isotopes revealed an extremely linear relationship. Thus, an arbitrary intensity cutoff for $^{158}GdO^{+}$ of 200,000 was selected and the data filtered so that only spectra containing a $^{158}GdO^{+}$ peak above the cutoff remained.

Plots of the intensities of the isotopes and ratios of the isotopes with the filtered data were then generated. A Monte Carlo experiment was performed using the sum of the isotopes under the assumption that these variables follow a poisson distribution. One thousand isotope ratios were generated using this model. The mean, standard deviation, and 95% confidence interval of this data were generated.

RESULTS/DISCUSSION

Summary statistics and confidence intervals for the five datasets are shown below in Table 1.

Table 1: Summary Statistics of Natural Uranium Containing UO_2Cl_2 at Varying Concentrations with 50 ppm $GdCl_3$ Internal Standard

SAMPLE NUMBER	UO2 CONCENTRATION (PPM)	U-235/U-238 RATIO	STANDARD ERROR	2.5 PERCENTILE	97.5 PERCENTILE	95 PERCENTILE
1	50	NA	NA	NA	NA	NA
2	5	0.3449	0.00071	0.3435	0.3463	0.3461
3	0.5	0.515	0.00189	0.5114	0.5187	0.5181
4	25	0.01791	0.000015	0.01788	0.01794	0.01794
5	250	0.007312	0.0000067	0.007305	0.007330	0.007329

An arbitrary ion count threshold of 200,000 was established to filter low intensity data based on experience with PSI-MS data sets other than those provided in this report. Future work will involve the development a dynamic threshold based on signal-to-noise ratios of target peaks within MS data sets; this was not possible with the given data set due to a lack of blank spectra collected during a short vendor demonstration. Sample 1 contained no spectra containing a $^{158}GdO^+$ peak above a 200,000 ion count threshold; thus, the analysis was not be performed due to weak ion beam intensity. As one can see, the data differs significantly from the uranium literature isotopic ratio of 0.00727 at the .05 level. We believe that there are several reasons for this discrepancy, the most obvious being low ion beam intensity. A low signal-to-noise ratio (SNR) appears to be a significant impediment for Samples 2 and 3. Further investigation of the

data revealed no spectrum contained in Samples 2 or 3 with a $^{238}UO_2^+$ above 60,000, whereas Samples 4 and 5 contained many spectra with $^{238}UO_2^+$ peaks above 1,000,000 and 4,000,000, respectively. The low SNR is further highlighted below in Figure 1, which explicitly illustrates the large amount of noise present in the data.

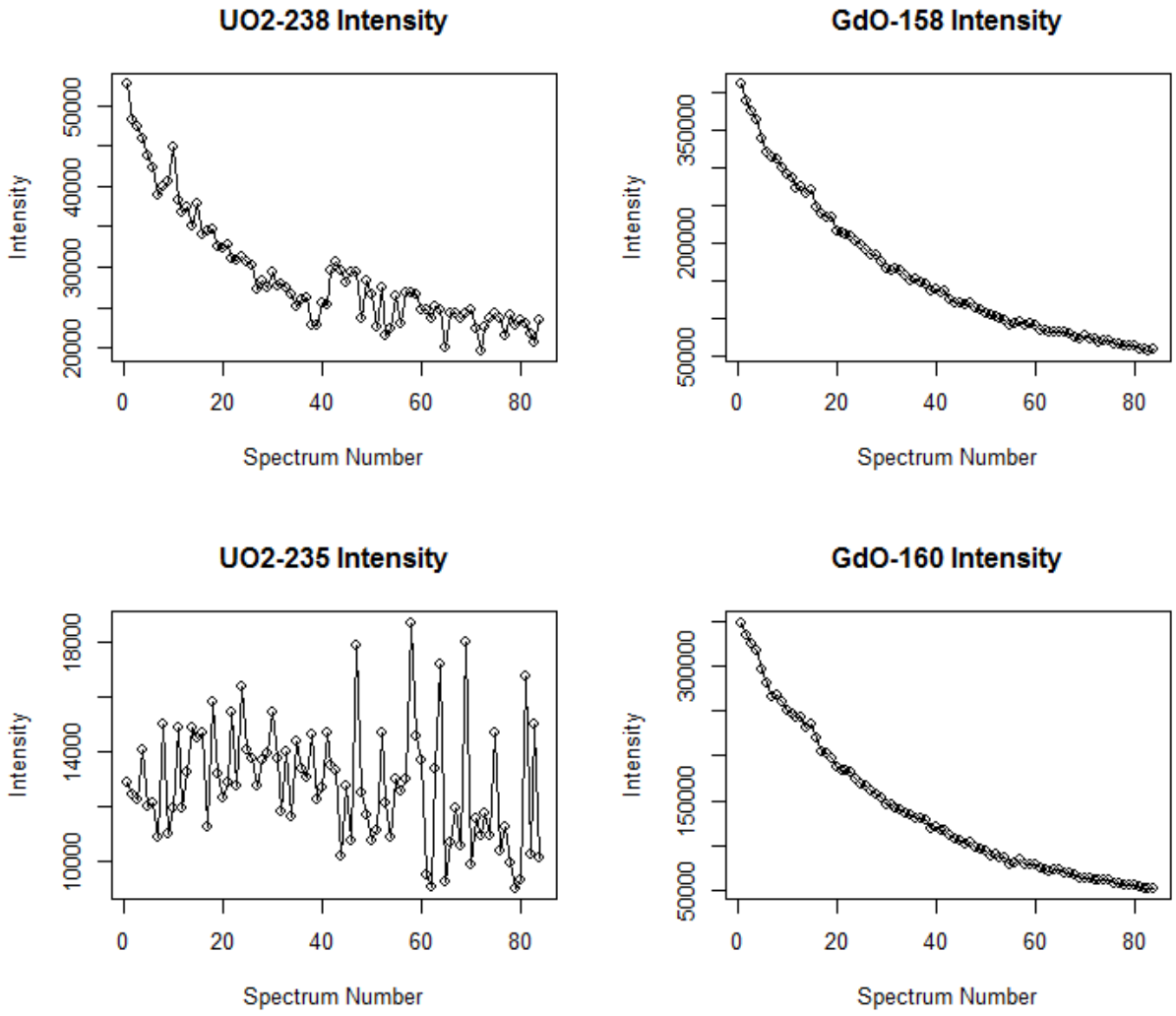

Figure 1: Relationship between analyte intensity and chronological spectrum within Sample 2. Each analyte displays a similar exponential relationship with Spectrum Number with the notable exception of $^{235}UO_2^+$, which has no discernable pattern and appears to be mostly noise.

As expected, the $^{158}GdO^+$ and $^{160}GdO^+$ intensities exhibit the exact same relationship with respect to the Spectrum Number. However, the two uranium isotopes exhibit remarkable

different patterns. As the intensity of the $^{238}UO_2^+$ decreases from approximately 50,000 to 25,000, the intensity of $^{235}UO_2$ remains relatively constant with large variations from point to point. This observation suggests that the $^{235}UO_2^+$ signal of this dataset is below the quantification threshold for this dataset, and thus will yield extremely unreliable results. Further examination of Sample 3, shown below in Figure 2, reveals a similar yet less pronounced trend in the data, whereby the $^{238}UO_2^+$, $^{158}GdO^+$, and $^{160}GdO^+$ peak intensities exhibit spikes and local maxima at or around the same Spectrum Number, yet the $^{235}UO_2^+$ peak intensities exhibit a large spike at Spectrum Number 62 that does not appear in the other peak intensities.

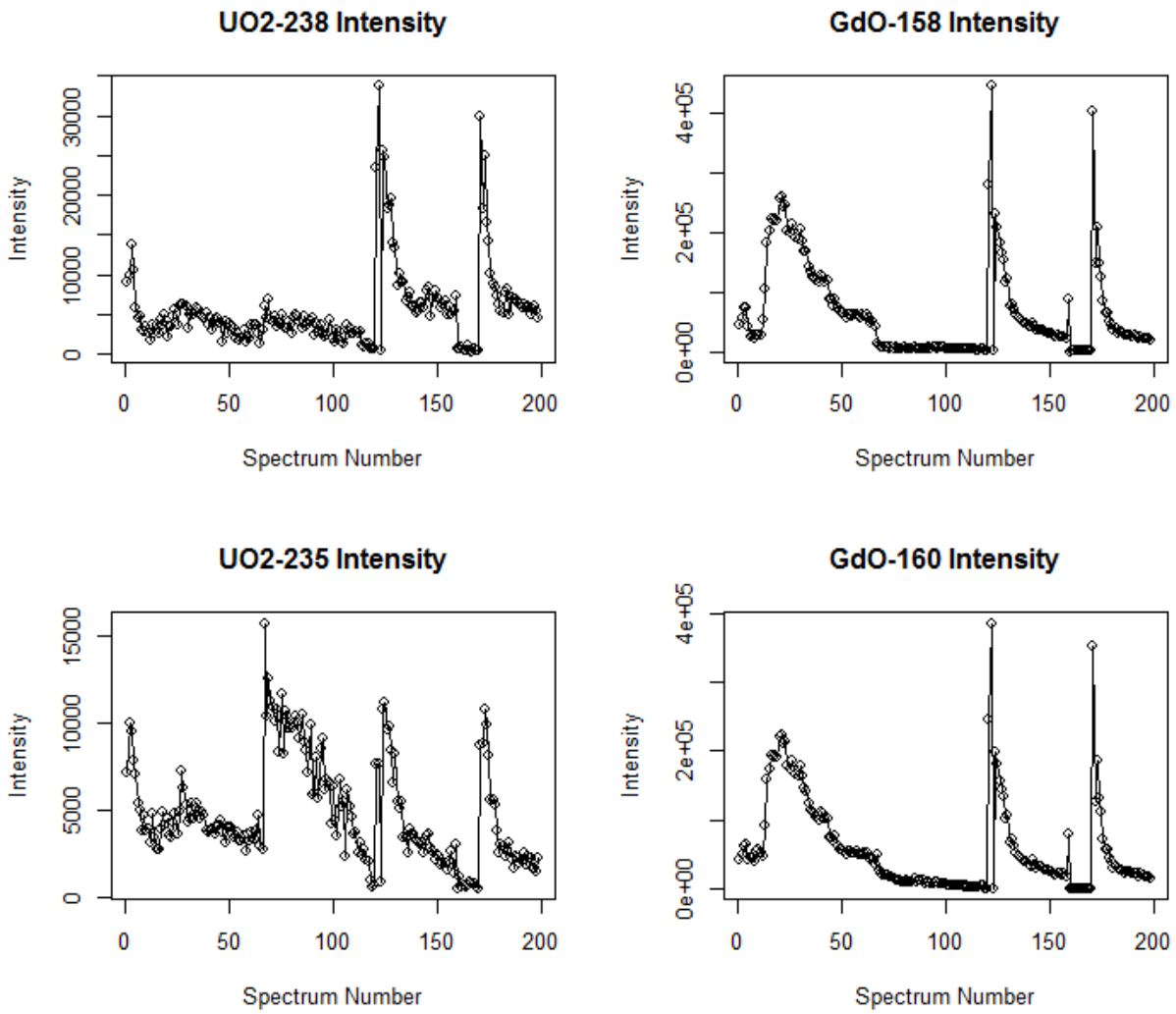

Figure 2: Relationship between analyte intensity and chronological spectrum within Sample 3. Each analyte displays a similar relationship with Spectrum Number, whereby local maxima are contained at or around the same Spectrum Number with the notable exception of $^{235}UO_2^+$, which contains a broad and large spike unseen in the other analytes.

Samples 4 and 5 do not display the pattern divergence with the $^{235}UO_2^+$ intensity peaks observed in Samples 2 and 3. As shown below in Figure 3, the $^{235}UO_2^+$ intensity peak distribution follows almost exactly that of the other analytes in both Samples 4 and 5, albeit with some additional variability.

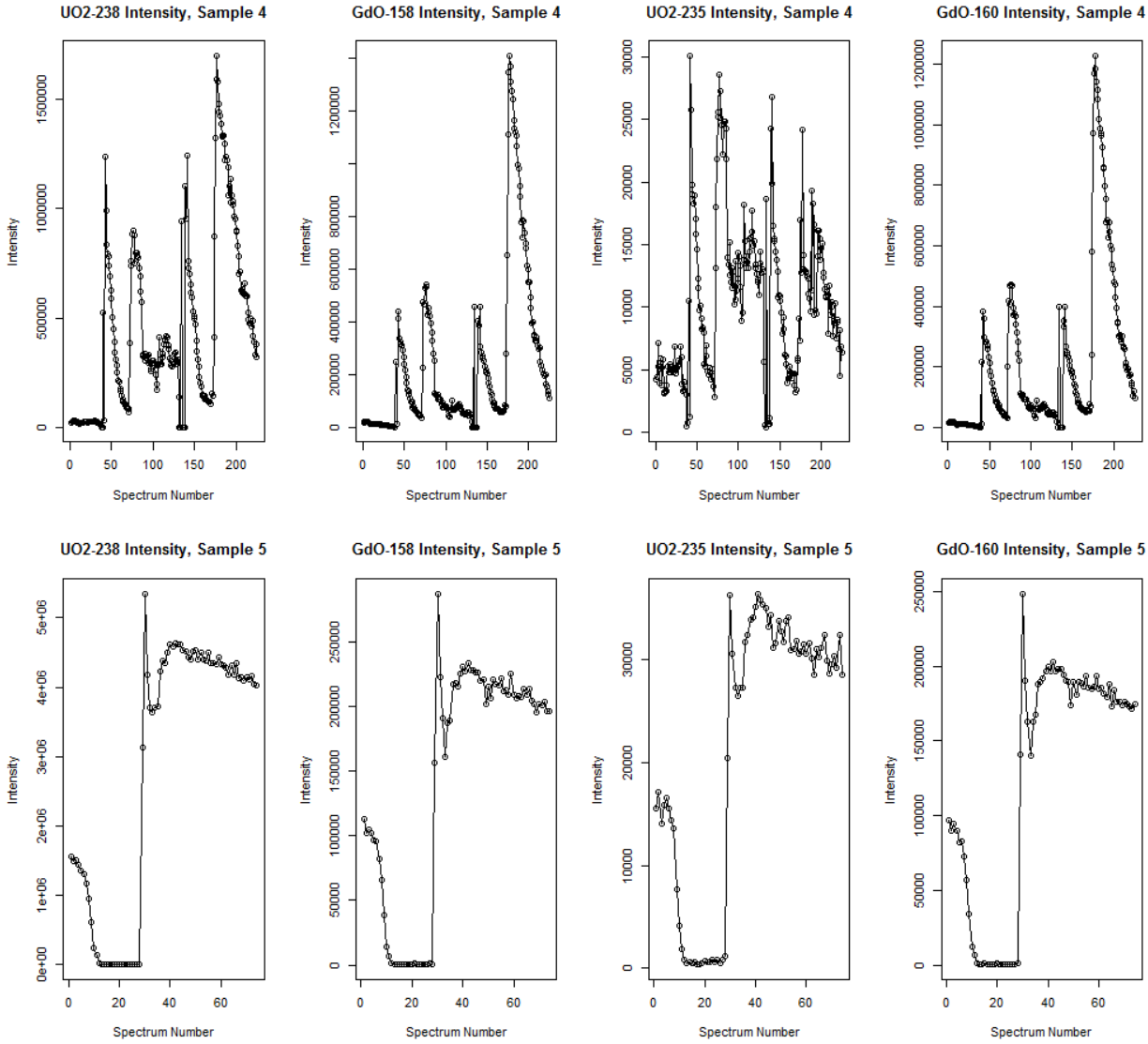

Figure 3: Relationship between analyte intensity and chronological spectrum within Samples 4 and 5. As opposed to Samples 2 and 3, the $^{235}UO_2^+$ intensity peak distribution of both Samples 4 and 5 almost exactly match the distribution of the other analytes with some additional variability.

As the isotopic ratio predictions obtained from Samples 4 and 5 are orders of magnitude closer to the true isotopic ratio of 0.007272, we believe that this low SNR is the main effect causing the poor results obtained from Samples 2 and 3. The underlying causes of the low SNR differs by sample. In the case of Sample 2, it appears reasonable that an instrumentation operation error is to blame. This explains the almost constant linear decrease in the total ion count with respect to time in Sample 2, as shown below in Figure 4.

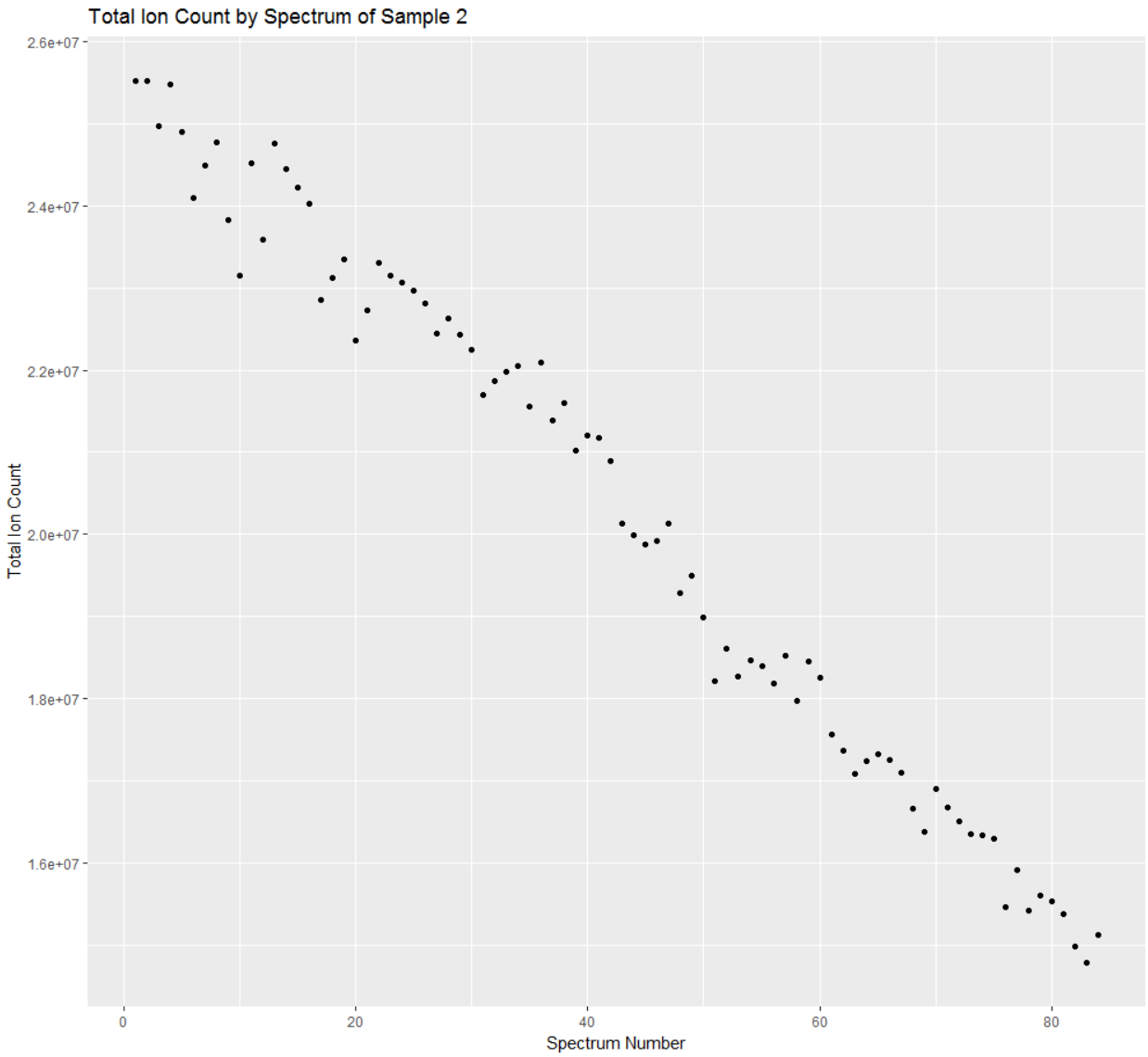

Figure 4: Total Ion Count versus Spectrum Number of Sample 2. Total Ion Count refers to the sum of the intensity values corresponding to every mass value contained within a given spectrum.

In the case of Sample 3, we believe the low SNR is due to the small concentration of UO_2Cl_2 analyzed in the experiment, which appears to be significantly below the limit of quantification for the instrument. This would explain the sufficiently high number of spectra with $^{158}GdO^+$ intensity peaks above the 200,000 threshold—19 peaks in total—with the erroneous prediction of approximately 33% enrichment. Simply put, almost all of the UO_2^+ intensity peaks of both isotopes are dominated by the noise.

Besides the low signal intensity, the lack of a sufficient estimate for the noise and signal caused by organic contaminants arising from the application of a high voltage to a paper substrate in ambient conditions is a significant barrier to producing accurate, reliable results. The presence of this noise will tend to increase our calculated uranium isotope ratio, as it has a higher leverage on smaller numbers than larger numbers. This explains why our ratio plots consistently center the data along the horizontal axis at a higher value than the literature value of the gadolinium ratio. The lack of this background data is due to the limited amount of time given to run experiments during the initial trial of the instrument. As we have not as of this time been able to install the instrument on site, this data is all that we have had to work with. We believe that once we are able to correct our estimates for the background noise and contaminant signal, our results for all samples improve, and specifically the results for Samples 4 and 5.

The data pipeline that we have designed appears fairly robust on initial testing. Upon visual inspection, the quality control plot produced by plotting the ratio of $^{235}UO_2^+$ and $^{238}UO_2^+$ by the ratio of $^{158}GdO^+$ to $^{160}GdO^+$ indicate that Samples 2 and 3 should all be excluded from further analysis due to the lack of a dense cluster of data points around the literature value of the ratio of the gadolinium isotopes, as seen in Figure 5.

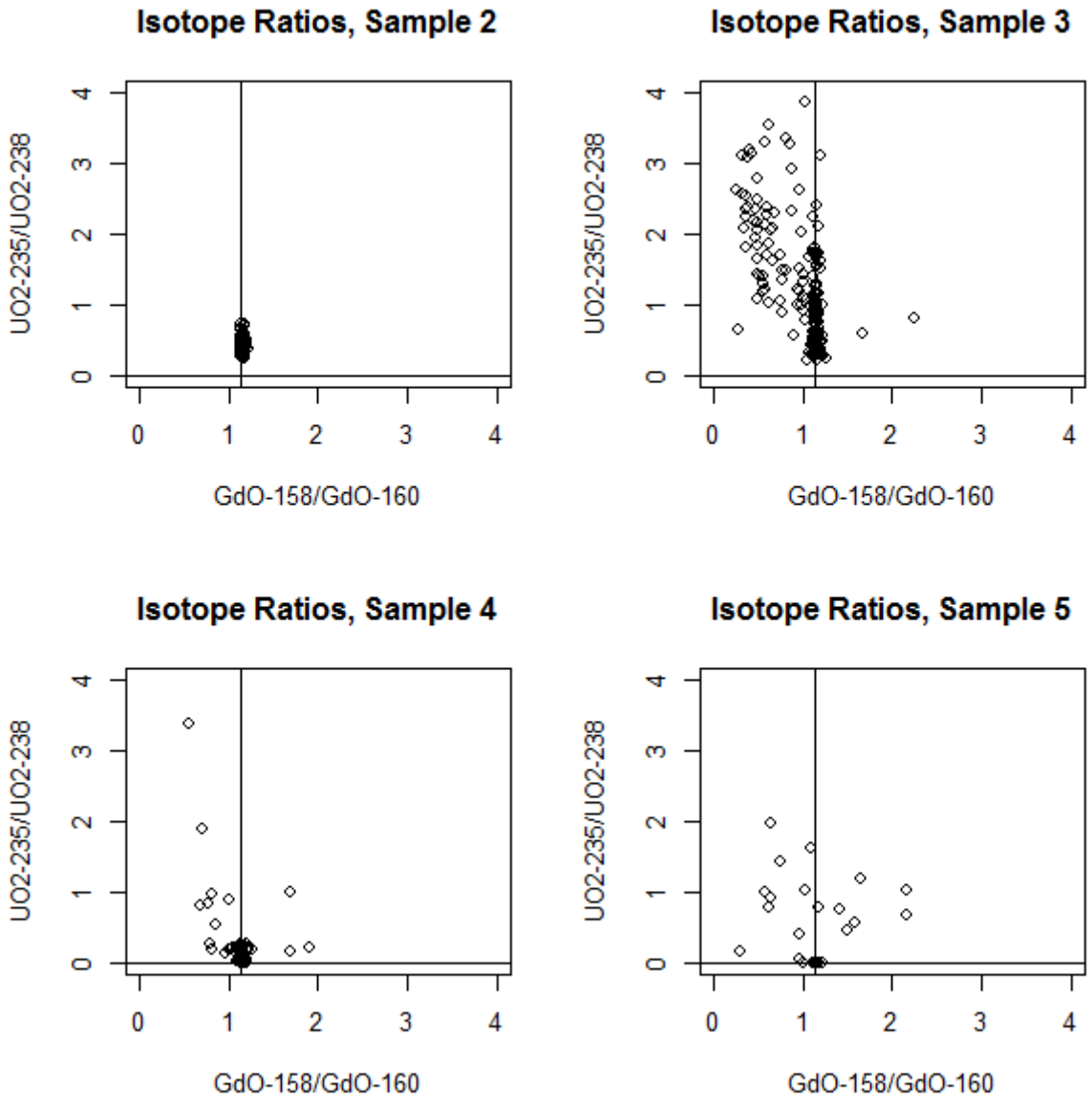

Figure 5: Uranium isotope ratios versus gadolinium isotope ratios. Note that the vertical line represents the literature value of the gadolinium isotope ratio while the horizontal line represents the literature value of the uranium isotope ratio.

The graphs of Samples 2 and 3 display dense clusters centered on the gadolinium ratio literature value with significant spread around the uranium isotope axis, while the graphs of Samples 4 and 5 display dense clusters around both the gadolinium and uranium isotope axes. This indicates

that the data is unstable in Samples 2 and 3, but stable in Samples 4 and 5 for the purposes of isotopic ratio calculations.

CONCLUSIONS

The data presented above strongly supports the idea that the JEOL AccuTOF™-DART® LP 4G with a Filter Spray™ front end sample injection system may be used as a time and cost effective method for detection of trace quantities of UO_2Cl_2. At all UO_2Cl_2 concentrations where usable data was obtained, the ratio of $^{235}UO_2^+$ to $^{238}UO_2^+$ was significantly less than 1.0 at the .05 level, as seen in Table 1. If there was no UO_2^+ present and the response was purely noise, we would expect that the ratio of the two mass channels would be approximately 1.0, assuming that no contaminants were systematically detected at a significantly higher level at one of the mass channels. The data also supports the concept that the JEOL AccuTOF™-DART® LP 4G with a Filter Spray™ front end sample injection system may be used for isotopic ratio quantification of trace quantities of UO_2Cl_2. We have shown that at the 250 ppm concentration, the true isotopic ratio may be quantified to within 0.65% of the literature value for UO_2Cl_2 containing natural uranium. Though the accuracy of the prediction decrease rapidly with the concentration of UO_2Cl_2, we believe that improving our data collection protocol along with the quantification of a noise value and the implementation of noise-corrected ratios of intensity sums will greatly increase the accuracy of our results, leading to the use of this instrument for isotopic ratio quantification at lower concentrations of UO_2Cl_2.

The data pipeline that we have engineered has performed well on all samples used in this project. It has successfully distinguished high and low quality samples and made isotopic ratio predictions of within .1 of the literature value for each high quality sample. However, our

pipeline fails when there are no spectra containing high intensity peaks at the $^{158}GdO^{+}$ mass channels. We believe that this situation is a function of instrumental or operational error and not a realistic situation that will arise during proper instrumental operation. However, if in fact this prediction is not valid, we will have to review our data filtration threshold.

Future work on our data pipeline should focus on generalization and automation of our script, so that it may handle the analysis of compounds other than UO_2Cl_2. This would allow us to test our analysis on other uranium isotopes and oxidations states, as well as on compounds containing other actinides. Furthermore, we would like to test our analysis on UO_2Cl_2 containing both enriched and depleted uranium. These experiments would demonstrate the generalizability of our analysis pipeline beyond simple UO_2Cl_2 containing natural uranium.

ACKNOWLEDGEMENTS

I would like acknowledge and mentor, Dr. Matthew Wellons, for his consistent assistance and guidance throughout this project, and Dr. Joseph Mannion and Dr. Joshua Hewitt. I would also like to acknowledge the authors of the MALDIquant and MALDIQUANT packages, Sebastian Gibb and Korbinian Strimmer, and the author of the ncdf4 package, David Pierce. Finally, I would like to acknowledge the Department of Energy and the Savannah River National Laboratory for funding and housing my project.

APPENDIX

Data Analysis Pipeline

Loading Data and 3D Visualization

Data is ingested into the pipeline and parameters are given, specifically the concentration of uranium analyte and the background noise. Note that noise is set to 0 for this demonstration. 3D plots are generated from this data.

```
library(MALDIquant)

##
## This is MALDIquant version 1.17
## Quantitative Analysis of Mass Spectrometry Data
##  See '?MALDIquant' for more information about this package.

library(MALDIquantForeign)
library(tidyverse)

## -- Attaching packages ---------------------------------------------------
------------------------------------------------------------ tidyverse 1.2.1
--

## v ggplot2 2.2.1     v purrr   0.2.5
## v tibble  1.4.2     v dplyr   0.7.5
## v tidyr   0.8.1     v stringr 1.3.1
## v readr   1.1.1     v forcats 0.3.0

## -- Conflicts ------------------------------------------------------------
------------------------------------------------------- tidyverse_conflicts()
--
## x dplyr::filter() masks stats::filter()
## x dplyr::lag()    masks stats::lag()

library(plot3D)

gd=read.csv('C:/Users/J3421/Documents/Project Info/Instrament famaliarization
visit 20171114/Raw data from Visit/U.csv', header=TRUE) #inuput of csv file
ppm=25

nlist=importCdf("C:/Users/J3421/Documents/Project Info/Instrament famaliariza
tion visit 20171114/Raw data from Visit/UO2Cl2_demo_FS_25ppmpos_19.cdf", verb
ose=F) #Input of data files
noise=0

i=1
mass_values=rep(0, 10000000) #creating placeholder vector for mass
intensity_values=rep(0, 10000000) #creating placeholder vector for intensity
spectrum_number=rep(0, 10000000) #creating placeholder vector for the spectru
```

```
m number

for (j in 1:length(nlist)){
  for (k in 1:length(nlist[[j]])){
    mass_values[i]=mass(nlist[[j]])[k]
    intensity_values[i]=intensity(nlist[[j]])[k]
    spectrum_number[i]=j
    i=i+1
  }
}

mass_values=unlist(lapply(mass_values, function(x) if (x > 0) x)) #removing e
xtra 0s
intensity_values=unlist(lapply(intensity_values, function(x) if (x > 0) x))
spectrum_number=unlist(lapply(spectrum_number, function(x) if (x > 0) x))

lines3D(spectrum_number, mass_values, intensity_values, xlab="Time", ylab="M/
Z", zlab="Intensity", ticktype="detailed", nticks=2, cex.axis=.5) ## 3D line
graph
```

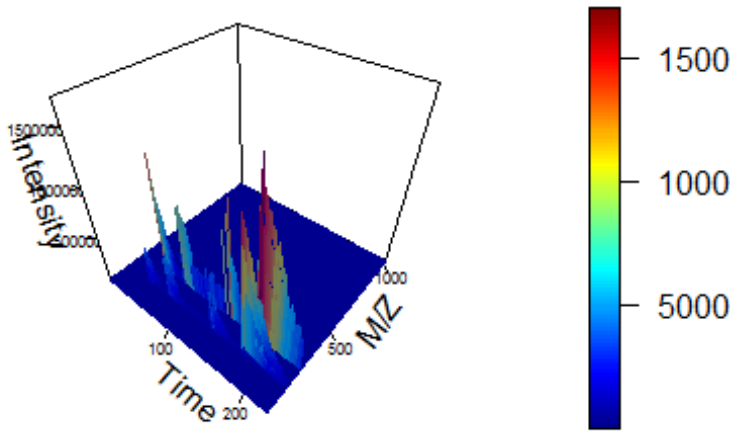

Extracting and Processing Intensity Values

Peak intensity values at each mass channel of interest are extracted. The ratios of the resulting vectors are used to build a data frame for the construction of a quality control plot.

```
values=list() #list of intensities for each spectrum by isotope
```

```
for (i in 1:nrow(gd)){ #loop through each isotope of interest
  a=rep(-Inf, length(nlist)) #creation of placeholding vector
  for (j in 1:length(nlist)){ #loop through each spectra
    m=mass(nlist[[j]]) #extracting mass values
    n=intensity(nlist[[j]]) #extracting intensity values
    a[j]=max(n[which(abs(m-gd$Mass[i]) <= .3)]) #determination of local maxim
a of intensity values
  }
  a=unlist(lapply(a, function(x) if (is.finite(x)) x else 0)) #postprocessing
to remove -Inf values
  values[[i]]=a
}
structure=data.frame(values)
colnames(structure)=paste(as.character(gd$Isotope), "Intensity") #Renaming Co
lumn names
attach(structure)
d1=data.frame(`UO2-235 Intensity`/`UO2-238 Intensity`, `GdO-158 Intensity`/`G
dO-160 Intensity`)
detach(structure)
colnames(d1)=c("UO2.Ratio", "GdO.Ratio")
```

Construction of Quality Control Plot

A plot of the ratios of the two isotopes is constructed for quality control purposes. We are seeking to filter out samples where data is not centered on the literature value of the ratio of the gadolinium isotopes, represented by the vertical line, and with high spread about the vertical axis. The literature value of the ratio of the uranium isotopes is represented by the horizontal line.

```
ggplot(data=d1, aes(`GdO.Ratio`, `UO2.Ratio`))+
  geom_point()+
  geom_hline(aes(yintercept=gd$Abundance[2]/gd$Abundance[1]))+
  geom_vline(aes(xintercept=gd$Abundance[3]/gd$Abundance[4]))+
  labs(title=paste("UO2 Ratio vs GdO Ratio,", ppm, "ppm"))
```

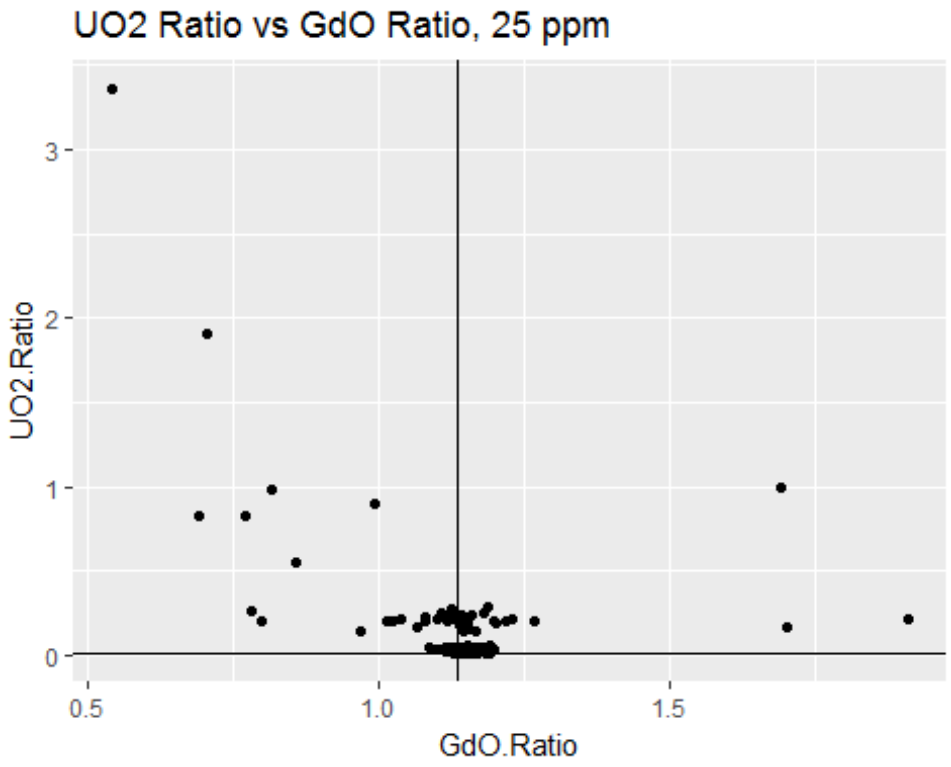

Data Filtration and Visualization

We apply a 200,000 peak intensity threshold to the GdO-158 mass channel as a means of filtering our data. We then plot the intensities of the isotopes of the two elements, expecting to see a strong linear relationship. Finally, we remake the previous quality control plot, this time with the filtered data.

```
gd.test=structure[structure$`GdO-158`> 200000, ]
attach(gd.test)

ggplot(data=gd.test, aes(`GdO-158 Intensity`, `GdO-160 Intensity`))+
  geom_point()+
  labs(title=paste("GdO-158 vs GdO-160, Filtered Data", ppm, "ppm"))
```

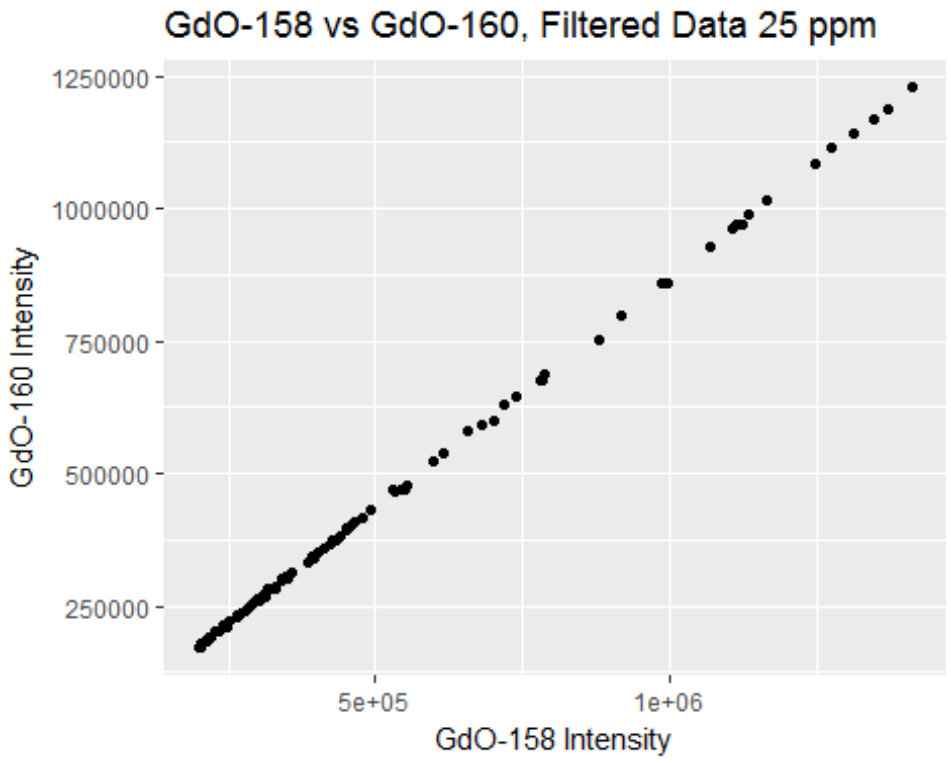


```
ggplot(data=gd.test, aes(`UO2-238 Intensity`, `UO2-235 Intensity`))+
  geom_point()+
  labs(title=paste("UO2-235 vs UO2-238, Filtered Data,", ppm, "ppm"))
```

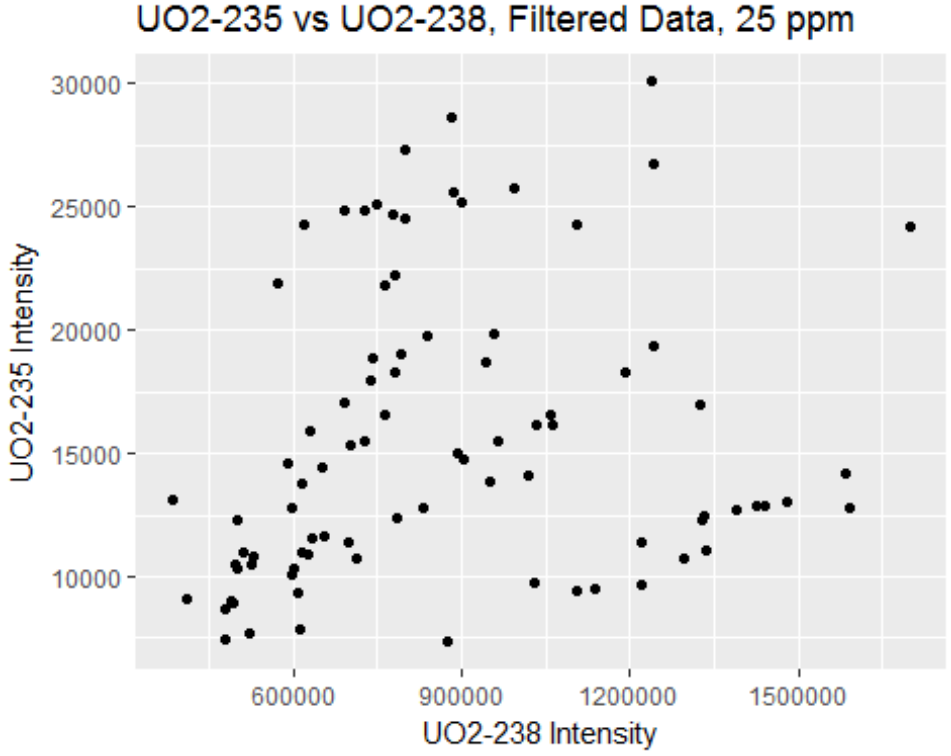

```
d2=data.frame(`UO2-235 Intensity`/`UO2-238 Intensity`, `GdO-158 Intensity`/`G
dO-160 Intensity`)
colnames(d2)=c("UO2.Ratio", "GdO.Ratio")
ggplot(data=d2, aes(`GdO.Ratio`, `UO2.Ratio`))+
  geom_point()+
  geom_hline(aes(yintercept=gd$Abundance[2]/gd$Abundance[1]))+
  geom_vline(aes(xintercept=gd$Abundance[3]/gd$Abundance[4]))+
  labs(title=paste("UO2 Ratio vs GdO Ratio, Filtered Data", ppm, "ppm"))
```

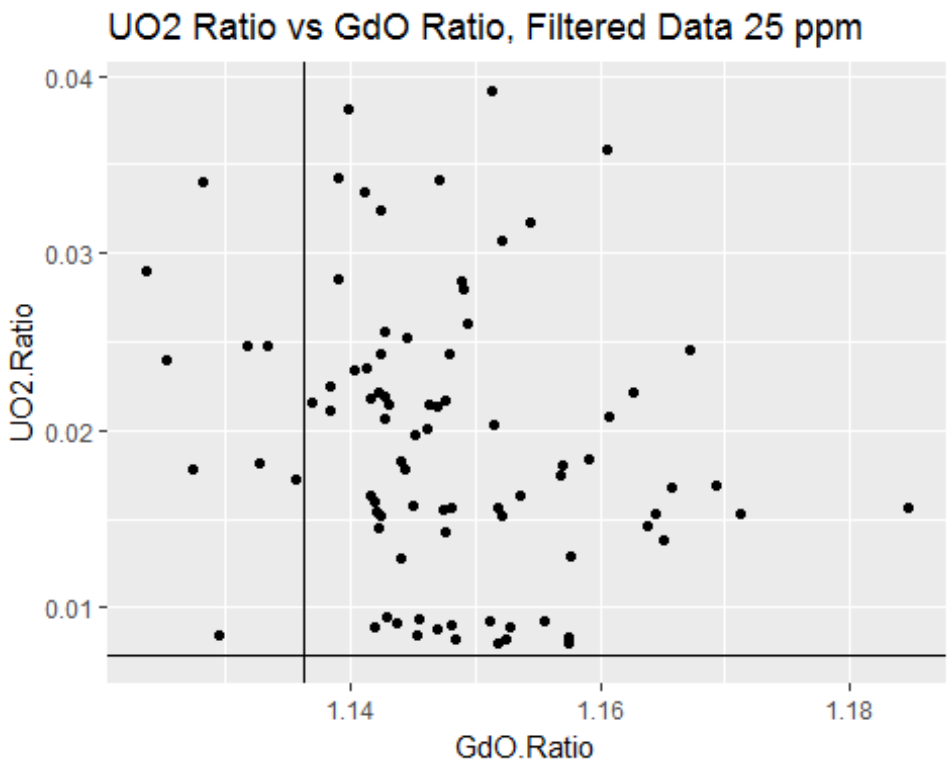

Monte Carlo Experiment and Ratio Prediction

We use a Monte-Carlo Experiment with the assumption that the peak intensities follow a poisson distribution to estimate the true ratio of the uranium isotopes. We then calculate summary statistics and confidence intervals using the theoretical data.

```
set.seed(5873)
a=`UO2-235 Intensity`-noise
b=`UO2-238 Intensity`-noise
mc.235=round(rnorm(10000, mean=sum(a), sd=sqrt(sum(a)))) #Creating theoretica
l distribution with normal approximation to poisson
mc.238=round(rnorm(10000, mean=sum(b), sd=sqrt(sum(b)))) #Creating theoretica
l distribution with normal approximation to poisson

mc.ratio=mc.235/mc.238 #Creating distribution of ratio
mean(mc.ratio)

## [1] 0.01791356
```

```
sd(mc.ratio)

## [1] 1.554943e-05

quantile(mc.ratio, c(.025, .975)) #Calculating two-sided 95% Confidence Inter
val for the true ratio

##       2.5%      97.5%
## 0.01788335 0.01794388

quantile(mc.ratio, .95) #Calculating upper bound of one-sided 95% Confidence
Interval for the true ratio

##        95%
## 0.01793921

detach(gd.test)
```

REFERENCES

1. J. Zheng, K. Tagami, Y. Watanabe, S. Uchida, T. Aono, N. Ishii, S. Yoshida, Y. Kubota, S. Fuma and S. Ihara, Scientific Reports **2**, 304 (2012).
2. J. S. Becker, M. Zoriy, L. Halicz, N. Teplyakov, C. Muller, I. Segal, C. Pickhardt and I. T. Platzner, J. Anal. At. Spectrom. **19** (9), 1257-1261 (2004).
3. K. Mayer, M. Wallenius and I. Ray, Analyst **130** (4), 433-441 (2005).
4. Y. Kimura, N. Shinohara and Y. Funatake, Energy Procedia **131**, 239-245 (2017).
5. M. Wallenius and K. Mayer, Fresenius' Journal of Analytical Chemistry **366** (3), 234-238 (2000).
6. D. Suzuki, F. Esaka, Y. Miyamoto and M. Magara, Applied Radiation and Isotopes **96**, 52-56 (2015).
7. S. Boulyga, S. Konegger-Kappel, S. Richter and L. Sangely, J. Anal. At. Spectrom. **30** (7), 1469-1489 (2015).
8. D. L. Donohue, J. Alloys Compd. **271–273**, 11-18 (1998).
9. A. R. Gillens and B. A. Powell, J. Radioanal. Nucl. Chem. **296** (2), 859-868 (2013).
10. S.-W. Hu, X.-Y. Wang, T.-W. Chu and X.-Q. Liu, The Journal of Physical Chemistry A **113** (32), 9243-9248 (2009).
11. S. K. Aggarwal, Anal. Methods **8** (5), 942-957 (2016).
12. R. N. Taylor, T. Warneke, J. A. Milton, I. W. Croudace, P. E. Warwick and R. W. Nesbitt, J. Anal. At. Spectrom. **16** (3), 279-284 (2001).
13. J. Švedkauskaite-LeGore, K. Mayer, S. Millet, A. Nicholl, G. Rasmussen and D. Baltrunas, in *Radiochimica Acta* (2007), Vol. 95, pp. 601.
14. R. D. Espy, S. F. Teunissen, N. E. Manicke, Y. Ren, Z. Ouyang, A. van Asten and R. G. Cooks, Anal. Chem. **86** (15), 7712-7718 (2014).
15. R.-Z. Shi, E. T. M. El Gierari, N. E. Manicke and J. D. Faix, Clinica Chimica Acta **441**, 99-104 (2015).
16. R. Jett, C. Skaggs and N. E. Manicke, Anal. Methods **9** (34), 5037-5043 (2017).
17. J. A. Michely, M. R. Meyer and H. H. Maurer, Anal. Chem. **89** (21), 11779-11786 (2017).
18. E. S. Jeong, K. H. Kim, E. Cha, O.-S. Kwon, S. Cha and J. Lee, Journal of Chromatography B **1028**, 237-241 (2016).

19. E. S. Dhummakupt, P. M. Mach, D. Carmany, P. S. Demond, T. S. Moran, T. Connell, H. S. Wylie, N. E. Manicke, J. M. Nilles and T. Glaros, Anal. Chem. **89** (20), 10866-10872 (2017).